Published in final edited form as:

J Immunol. 2016 December 1; 197(11): 4274–4282. doi:10.4049/jimmunol.1601207.

CD8αα$^+$MHC-II$^+$ Cell with Capacity to Terminate Autoimmune Inflammation Is A Novel Antigen-Presenting NK-Like Cell in Rats

Jean Wu[*], **Colin Carlock**[*,1], **April Ross**[*,2], **Junbo Shim**[*], and **Yahuan Lou**[*]

[*]Department of Diagnostic Sciences, University of Texas Health Science Center at Houston, Houston, TX 77054

Abstract

Discovery of immune tolerance mechanisms, which inhibit pre-existing autoimmune inflammation, may provide us with new strategies for treating autoimmune diseases. We have identified a CD8αα$^+$MHC-II$^+$ cell with professional APC capacity during our investigation on spontaneous recovery from autoimmune glomerulonephritis in a rat model. This cell actively invades inflamed target tissue and further terminates an on-going autoimmune inflammation by selective killing of effector autoreactive T cells. Now, we showed that this cell used a cytotoxic machinery of Ly49s$^+$ NK cells in killing of target T cells. Thus, this CD8αα$^+$MHC-II$^+$ cell was a dually functional antigen presenting NK-like (AP-NK) cell. Following its coupling with target T cells through antigen presentation, killing stimulatory receptor Ly49s6 and co-receptor CD8αα on this cell used non-classic MHC-I RT1CE16 on the target T cells as a ligand to initiate killing. Thus, activated effector T cells with elevated expression of RT1CE16 were highly susceptible to the killing by the CD8αα$^+$ AP-NK cell. Granule cytolytic perforin/granzyme C from this cell subsequently mediated cytotoxicity. Thus, inhibition of granzyme C effectively attenuated the killing. As it can recognize and eliminate effector autoreactive T cells in the inflamed target tissue, CD8αα$^+$ AP-NK cell not only represents a new type of immune cell involved in immune tolerance, but also is a potential candidate for developing a cell-based therapy for pre-existing autoimmune diseases.

Keywords

APC; NK; immune tolerance; rat

Introduction

Most of autoimmune diseases are of inflammatory nature (1, 2). Autoreactive T cells are doubtless the most critical player in these diseases. These T cells function as effectors in both initiation and maintenance of autoimmune inflammation in the target organs (3,4). Current therapies for those diseases largely rely on non-specific anti-inflammatory

Correspondence: Dr. Yahuan Lou, Department of Diagnostic and Biomedical Sciences, SD, The University of Texas HSC at Houston, 5326 Behavioral and Biomedical Science Building (BBSB), 1941 East Road, Houston, TX 77054, Phone: 713-486-4059, Fax: 713-486-0450, Yahuan.lou@uth.tmc.edu.

[1]**Current address**: Department of Biochemistry, Purdue University, 175 South University Street, West Lafayette, IN 47907-2063

[2]**Current address**: Department of Immunology, University of Texas M.D. Anderson Cancer Center, Houston, TX 77030

medications, and thus, cannot permanently exterminate the inflammation often with undesirable serious side effects. Development of immunotherapies, which can specifically target autoreactive T cells, is a new hope on the horizon for treating inflammatory autoimmune diseases (5). Candidate immune cells for such therapies must be able to specifically silence or terminate a T cell-mediated autoimmune response or inflammation. To discover and elucidate novel immune tolerance mechanisms are the pre-requisite for identifying such candidate immune cells.

Many types of immune cells (e.g. Treg cells, immature or tolerogenic dendritic cells and a subset of NK cells) have been candidates for immunotherapies (6–9). These cells reside in lymphoid organs or normal tissues, and eliminate naïve auto-reactive T cells or deviate them to non-pathogenic phenotype. Thus, generation of effector autoreactive T cells and subsequent autoimmune inflammation are prevented *de novo*. However, pathogenic autoreactive T cells can evade these tolerance mechanisms through molecular mimicry or by-stander activation during infections (10, 11). Are there any last ditch tolerance mechanisms that suppress autoimmunity after pathogenic autoreactive T cells have caused or are causing tissue damage? To address this fundamental question is critical for both our full understanding of immune tolerance and development of immunotherapies. Clinically, it is difficult to detect autoimmune diseases before their onset. A practical therapy is to suppress a pre-existing disease rather than to prevent them. Therapeutic strategies based on many tolerance mechanisms may successfully prevent the diseases, but are less effective for treating a pre-existing disease.

During our investigation on spontaneous recovery from autoimmune glomerulonephritis in Lewis (LEW) rats, a population with CD8αα$^+$MHC-II(RT1B/D)$^+$ phenotype and professional APC capacity has been identified (12–14). This population expands upon autoimmunization, and migrates into inflamed target tissue (13). Their Ag presentation induces apoptosis in effector autoreactive T cells in the target tissue, leading to a spontaneous recovery (14). We have linked migration deficiency to disease susceptibility in the disease-prone Wista Kyoto (WKY) rats. Significantly, transfer of this cell population of LEW rats attenuates pre-existing disease in WKY rats (15). This suggests that the CD8αα$^+$RT1B/D$^+$ cell is a potential candidate for immunotherapy for a pre-existing autoimmune disease. The present study aimed to investigate cytotoxic mechanisms in the CD8αα$^+$RT1B/D$^+$ cell. Our results showed that the CD8αα$^+$RT1B/D$^+$ cell was an unusual Ag presenting NK-like cells: it engages with and recognizes autoreactive effector T cells as an APC, and further kills them as an NK cell.

Materials and Methods

Rats and induction of glomerulonephritis

All procedures involving animals in this study were approved by the institutional animal welfare committee. Female WKY or LEW rats (4–6 weeks of age) were purchased from Harlan (Indianapolis, IN). Rats were immunized with peptide pCol(28–40) (0.15 μmol) emulsified in complete Freund Adjuvant, in one hind footpad and at the base of the tail (10). Development of proteinuria in these rats was closely monitored daily. Immunized rats were then used for the isolation of various leukocyte populations at day 30–35 depending on their

status of proteinuria. Peripheral blood and kidneys were removed under a sterile condition for cell isolation. A portion of renal tissues were either snap frozen or fixed for evaluation of renal pathology. In some cases, immunized rats were perfused with 2% of paraformaldehyde for *in situ* hybridization.

Abs

Biotin labeled anti-rat CD3 (G.4.18), PE-labeled anti-rat CD4 (OX35), CD8α (OX8), CD11c, RT1B (OX6), FITC labeled anti-rat CD8α, RT1B (OX6), RT-1D (OX17), and APC-labeled CD8α were from BD Biosciences (San Diego, CA). Goat anti-CD34, CD94 and rat NK marker (ANK61), anti-rat granzyme C were from Santa Cruz Biotechnology (Sana Cruz, CA). Anti-rat CD32 (D34–485) was used for Fc block. PE, FITC, anti-rat IgG, and purified rat IgG were from Southern Biotechnology (Birmingham, AL). Various mouse Ig isotypes (BD Biosciences, San Diego, CA) and normal rat/mouse IgG (Southern Biotechnology) were used as controls in both flow cytometry and immunofluorescence. Anti-Ly49s antiserum was generated through immunization of mice with a synthetic 16-mer peptide of conserved region of Ly49s receptors (DCGKRYLCICEKGMDK). Sera from mice immunized with adjuvant alone or an irrelevant peptide were used as negative controls.

Isolation and characterization of CD8αα$^+$RT1B/D$^+$ cells

PBMC fractions were first isolated from immunized rats by Ficoll gradient centrifugation. Glomeruli were purified from immunized rats and digested to release glomeruli-infiltrating leukocytes following a previously established method (14,15). The cells were subjected to isolation of various cell populations on a magnetic beads-based automatic cell sorter (Miltenyi Biotec, Germany). Pan T cells were first removed by a pan-T cell isolation kit from the same company. CD8α$^+$ cells were then positively selected, and further fractionated into RT1B/D^{high} and RT1B/D^{low} populations using a combination of removable anti-fluorescence Ab and FITC-anti-RT1B/D Ab (Miltenyi). All populations were then analyzed for their purities by 3-color flow cytometry (CD8α vs RT1B/D vs CD3). CD8α$^+$RT1B/D^{low} cells were further analyzed with two Abs to rat NK cells. Total 11 isolations were performed. Only those with purities above 93% were used for DNA microarray studies. Cells were either immediately used for isolation of total RNA, or fixed for immunofluorescence and *in situ* hybridization. Glomeruli-infiltrating CD8α$^-$RT1B/D$^+$ cells were considered as infiltrating macrophages. Thus, in addition to CD8αα$^+$RT1B/D$^+$ cells, the following populations were also obtained as controls: PBMC pan T cells, glomeruli-infiltrating macrophages and pan T cells.

Rat DNA microarray assay

Total RNA from various cell populations were isolated with a kit (Ambion, Austin, TX) and checked for their quality. Three hundred ng of total RNA were amplified and purified using Illumina TotalPrep RNA Amplification Kit (Illumina, San Diego, CA) following kit instructions. RNase H and DNA polymerase master mix were immediately added into the reaction mix following RT and were incubated for 2 hours at 16 ºC to synthesize second strand cDNA. *In vitro* transcription was performed and biotinylated cRNA was synthesized by 14-hour amplification with dNTP mix containing biotin-dUTP and T7 RNA polymerase. Amplified cRNA was subsequently purified and the concentration was measured by

NanoDrop ND-1000 Spectrophotometer (NanoDrop Technologies, Wilmington, DE). An aliquot of 750 ng of amplified products were loaded onto Illumina Sentrix Beadchip Array Rat arrays, hybridized at 58ºC in an Illumina Hybridization Oven (Illumina) for 17 hours, washed and incubated with streptavidin-Cy3 to detect biotin-labeled cRNA on the arrays. Arrays were dried and scanned with BeadArray Reader (Illumina). Data were analyzed using GenomeStudio software (Illumina). Clustering and pathway analysis were performed with GenomeStudio and Ingenuity Pathway Analysis (Ingenuity Systems, Redwood City, CA) softwares respectively. DNA microarray mega-data has been published (Access number GSE87099[NCBI tracking system #18061818] https://urldefense.proofpoint.com/v2/url?u=http-3A__www.ncbi.nlm.nih.gov_geo)

RT-PCR, molecular cloning and in situ hybridization (ISH)

Total RNAs from various cell populations were used for RT-PCR. cDNA was synthesized using 1 μg of total RNA through an RT kit (RNA PCR Core Kit, Applied Biosystems, Foster City, CA). Primers for various PCRs are listed in Table 1. qPCR for RT1CE16 on various T cells was performed under a similar condition as for conventional PCR using SYBR Green system (SuperArray Bioscience, Frederick, MD) on iCycler-iQ thermocycler (BioRad, Hercules, CA). Relative abundance was calculated as $2^{\Delta(t\text{-}t0)} \times 100(\%)$ with activated T cells or *Gapdh* as t_0. RNAs from isolated glomeruli of WKY rats at day 20 and 30 post immunization were used for RT^2 Profiler™ PCR Array rat apoptosis (QIAGEN, Hilden, Germany) following manufacture's instruction. For cloning of full length rat *gzm c*, full length of *ly49s6*, and degenerative cloning of intracellular/transmembrane domain of Ly49 receptors, RNA from glomeruli-infiltrating CD8αα$^+$RT1B/D$^+$ cells was used. RT-PCR products were cloned into pCR™-Blunt II-TOPO® vector (Invitrogen, Carlsbad, CA). Insert DNA from each clone was sequenced with either forward or reversed M13 promotor (Integrated DNA technologies, Coralville, IA). For ISH, paraformaldehyde-fixed cells or perfused renal tissues were used. Sense and antisense RNA for rat *gzm c* were transcribed from linearized plasmid containing full length rat *gzm c* with a transcription kit (MEGAscript®T7, Ambion, Austin, TX), using T7 or SP6 RNA polymerase, respectively; biotin-UTP was added at 25% of total UTP for labelling of RNA probes. Biotin-labeled RNA probes were then used for SSC/Denhardts based hybridization at 37°C with RNA probe (400ng/ml) in an ISH moisture chamber. After hybridization, cells or tissues were incubated with streptavidin-Texas Red, followed by immunofluorescence for RT1B/C or CD8α.

Immunofluorescence and flow cytometry

Fixed or live cells were used for immunofluorescence or flow cytometry following our previously published methods (12). For flow cytometry, standard controls included Ig isotypes and fluorescence minus one (FMO). For detection of intracellular Fas-L or gzm C, cells were permeablized with a regent (intracellular cytokine detection kit, BD Biosciences, San Diego, CA) before staining. All sections or cells were counter-stained by DAPI and observed with a digital fluorescent confocal microscope (Eclipse 80i, Nikon, Tokyo, Japan). Digital images were recorded for evaluation. Stained cells were also analyzed by a flow cytometry following our established method (14).

In vitro killing assays

T cell lines specific to pCol(28–40) were generated following our established method (14). Resting or activated T cells were used as target cells. For activation, T cells were incubated with irradiated thymic APC and pCol(28–40) at sub-optimal concentration (3μM) for 48 hours (14). In either cases T cells were then labelled by CFSE (15). Glomeruli-infiltrating CD8αα$^+$RT1B/D$^+$ were isolated as described above and used as killing effectors. To each of round-bottomed well of 96-well plate, 10^5 labeled T cells and 10^5 CD8αα$^+$RT1B/D$^+$ cells were added in the presence of 10μM pCol(28–40). In some cases, an Ab (2μg/ml) or normal IgG was added as indicated. Wells with T cells alone were used as a baseline for T cells number. Each set of incubation was duplicated. Remaining T cells were counted under a fluorescence microscope at 72 hours, and killing efficacy for each well was calculated as ratio (%) between T cell numbers of testing well vs T cells alone well.

Statistical analysis

Non-paired *t*-tests or linear regression were performed for comparison between various experimental results. One-way ANOVA with Tukey post test was used for comparison among >2 groups. Linear regression was used for analyze RT1CE16 expression and killing efficacy. p value < 0.05 was considered significant.

Results

A distinct global gene expression pattern of CD8αα$^+$RT1B/D$^+$ cells

We have shown a small size of the CD8αα$^+$MHC II(RT1B/D)$^+$ population in both peripheral blood mononuclear cells (PBMC) and glomeruli infiltrating leukocytes. A special magnetic beads-based cell sorting was first developed to maximize the purity and to minimize the damage to the cells (Fig. 1A, B). Two subpopulations, CD8αα$^+$RT1B/D^{high} and CD8αα$^+$RT1B/D^{low}, were obtained from each source (Fig. 1B). To separate into two subpopulations ensured free of potential contamination of CD8$^+$MHC-II$^-$ cells such as cytotoxic T, NK or γδT cells in CD8αα$^+$RT1B/D^{high} subset. Glomeruli-infiltrating macrophages and T cells, and PBMC T cells from the same individual were used as controls for comparisons (Fig. 1B). Global gene expression patterns of various CD8αα$^+$RT1B/D$^+$ subpopulations were analyzed by two independent DNA microarrays, with each containing two independent samples (total four) for each subpopulation. Both microarray showed that all CD8αα$^+$RT1B/D$^+$ subpopulations clustered together tightly (Fig. 1C), suggesting a similarity in their gene expression pattern. In contrast, glomeruli-infiltrating macrophages and pan T cells showed very distinct expression patterns (Fig. 1C). Thus, all CD8αα$^+$RT1B/D$^+$ subpopulations likely belonged to a single population, probably at different activation status. We used CD8αα$^+$RT1B/D^{high} subpopulation for the majority of experiments in this study unless indicated. These cells will be called as *CD8αα$^+$RT1B/D$^+$ cells*.

CD8αα$^+$RT1B/D$^+$ cells express genes associated with professional APCs and NK cells

We have previously reported that APC function of the CD8αα$^+$RT1B/D$^+$ cell is a prerequisite for induction of apoptosis in effector T cells (14). We analyzed the DNA

microarray data for the expression of gene clusters, which are associated with professional APC and apoptosis-related cytotoxicity. The CD8αα$^+$RT1B/D$^+$ cells expressed both professional APC- and NK cell-specific genes (Figure 1D). These APC related genes included MHC class II *rt1b/d/m*, invariant chain *Ii/clip* and proteases cathepsins, which are specific for Ag processing/presentation in professional APCs (Fig. 1E). The expression pattern of these genes in the CD8αα$^+$RT1B/D$^+$ cells was very similar to that of glomeruli-infiltrating macrophages, although the expression levels were lower (Fig. 1E). Reverse transcription (RT)-PCR on selected genes demonstrated that both CD8αα$^+$RT1B/D^{high} and CD8αα$^+$RT1B^{low} subsets expressed *rt1ba* and *Clip*/*li* (Fig. 1F). Thus, the CD8αα$^+$RT1B/D$^+$ cells possessed Ag processing/presentation apparatus for a professional APC as we have previously reported (14, 15). In fact, both α and β chains of *rt1b* and *rt1d* have been cloned from the CD8αα$^+$RT1B/D$^+$ cells (*GenBank AY701537-AY701540*). We next analyzed the expression of NK associated genes, i.e. various NK killing stimulatory/inhibitory receptors, associated signaling proteins such as DAP12, and granule cytolytic proteins in the CD8αα$^+$RT1B/D$^+$ cells. The CD8αα$^+$RT1B$^+$ cells expressed nearly half of these genes at a significant level (Fig. 1D). Also, it is worthwhile to mention that the cells expressed an extremely high level of *Tyrobp* (Fig. 1D), which encodes DAP12, a known critical signaling molecule for killing receptor-mediated cytotoxicity in NK cells (16). DAP12's expression was further verified by RT-PCR (inset in Fig. 1D). Thus, the CD8αα$^+$RT1B/D$^+$ cells also expressed genes associated with NK cytotoxicity.

CD8αα$^+$RT1B/D$^+$ cells express NK killing stimulatory receptor Ly49s6 and cytolytic proteins

Three groups of molecules, i.e. killing activating/inhibitory receptors, granule cytolytic proteins and fas-L, are associated with NK cytotoxicity (17). *First*, we focused on the NK receptors. Two NK cell subsets i.e. Ly49$^+$ and NKR-P1B$^+$ have been identified in rats (18). The microarray revealed a predominant expression of NK receptors *Ly49* family, but not *Klrb1* family, in CD8αα$^+$RT1B$^+$ cells (Fig. 2A). The cells especially lacked the expression of *Klrb1b*, which encodes hallmark NKR-P1B for the NKR-P1B$^+$ subset. Thus, NK receptor expression pattern of CD8αα$^+$RT1B/D$^+$ cells resembled that of Ly49s$^+$ subset. Rat Ly49 family has at least 35 members, and their complicated expression pattern is associated with the host's MHC haplotypes (19). Furthermore, majority of them have not been studied or cloned in rats. RT-PCR indeed revealed a complicated expression pattern in CD8αα$^+$RT1B/D$^+$ cells including splice variants (Fig. 2B). However, PCR results did not match to those from the microarray, because the microarray covered only a few known Ly49 receptors from PVG strain. In addition, similarity among Ly49 members may have led to cross reactivity. Thus, both PCR and the microarray data may not accurately reflect real expression of Ly49 NK receptors. We decided to analyze intracellular/transmembrane domain of Ly49s, which determines if engagement of a receptor leads to killing activation or inhibition. Degenerative cloning of transmembrane/intracellular domain of Ly49 was performed with mRNA from the CD8αα$^+$RT1B/D$^+$ cells (lower panel, Fig. 2B). Amino acid sequences from 33 clones were then compared to known stimulatory or inhibitory Ly49 receptors (19, 20). All these sequences belonged to stimulatory receptors, with 18 being Ly49s6. No T-TYT-H motif for inhibitory receptors was observed in all these clones (20). Cloning of full-length cDNA from the CD8αα$^+$RT1B/D$^+$ cell showed that it was a novel

splice variant of killing stimulatory Ly49s6 with addition of 9 nucleotides (cDNA sequence GeneBank:*KX501213.1*) (Fig. 2C). With an Ab against C-terminal region of Ly49s6, co-expression of surface Ly49s6 and RT1B/D was demonstrated on the CD8αα$^+$RT1B/D$^+$ cells by both immunofluorescence and flow cytometry (Fig. 2D, E). These results provided direct evidence for the co-expression of NK- and professional APC-specific molecules in the CD8αα$^+$RT1B/D$^+$ cells. Thus, phenotype of this cell is *CD8αα$^+$RT1B/D$^+$Ly49s6$^+$*.

Second, we investigated the expression of cytolytic granule proteins. RT-PCR first detected abundant mRNAs for perforin (*pfr*) and granzymes (*gzm*) in the CD8αα$^+$RT1B/D$^+$Ly49s6$^+$ cells (Fig. 3A). Unlike NK and CD8$^+$ T cells, the CD8αα$^+$RT1B$^+$Ly49s6$^+$ cells preferentially expressed *gzm c* (Fig. 3A). cDNA encoding full length of *gzm c* (248a.a. with MW 28kD) was cloned from CD8αα$^+$RT1B$^+$Ly49s6$^+$ cells (GenBank:*KT878764.1*). Sequencing of independent clones confirmed it to be rat *gzm c*. ISH combined with immunofluorescence revealed *gzm c* mRNA in PBMC and glomeruli-infiltrating CD8αα$^+$RT1B$^+$Ly49s6$^+$ cells (Fig. 3B–D). Three-color immunofluorescence (RT1B, CD8α and Gzm C) demonstrated cytoplasmic Gzm C protein in these cells (Fig. 3E). Western blot detected Gzm C as 56kD protein instead of predicted 28kD (Fig. 3F). Gzm C is much less studied, and its native tertiary structure remains unclear. Our result agreed with a previous X-ray study that native Gzm C is a homodimer (21). Glomeruli-infiltrating CD8αα$^+$RT1B$^+$Ly49s6$^+$ cells, which were T cell killer, showed much higher level of Gzm C protein than other subpopulations (Fig. 3F).

Third, simultaneous expression of Fas-L with other cytotoxicity-related genes in NK or cytotoxic T cells is well known. We next asked if Fas-L was also expressed in the CD8αα$^+$RT1B$^+$Ly49s6$^+$ cells. With purified glomeruli from immunized rats, quantitative PCR (qPCR) array for apoptotic pathway revealed a 15-fold increase in glomerular *Faslg* expression at day 35 (the peak time for T cell apoptosis in glomeruli) as compared to day 20 (early inflammation)(13) (Fig. 4A). RT-PCR using fractionated cell populations demonstrated that the glomeruli-infiltrating CD8αα$^+$RT1B$^+$Ly49s6$^+$ cells were the source of glomerular *fasgl* but not for *LTα* (Fig. 4B). Flow cytometry on freshly purified glomeruli-infiltrating CD8αα$^+$RT1B$^+$Ly49s6$^+$ cells failed to detect Fas-L. However, permeabilization of the cells led to detection of Fas-L in 68% of these cells (Fig. 4C), suggesting the presence of intracellular Fas-L. Similarly, immunofluorescence detected Fas-L only in permeabilized CD8αα$^+$RT1B$^+$Ly49s6$^+$ cells (Fig. 4D). Intracellular Fas-L has been described as a “safe storage” through posttranslational modification, which is ready for mobilization upon stimulation (22).

Cytolytic granzyme C in CD8αα$^+$RT1B$^+$Ly49s6$^+$ cells mediates killing of autoreactive T cells

The above results demonstrated that the CD8αα$^+$RT1B$^+$Ly49s6$^+$ cell possessed both NK killing receptors/cytolytic granules and intracellular Fas-L. We next determined which pathway played a major role in killing autoreactive T cells. Three autoreactive T cell lines specific to autoantigen pCol(28–40) were activated with irradiated thymic APCs and pCol(28–40) for 48 hours; the T cells were harvested and labeled with CFSE as target cells. The target T cells were incubated with freshly isolated glomeruli-infiltrating

CD8αα$^+$RT1B$^+$Ly49s6$^+$ cells as killing effectors in the presence of pCol(28–40). Anti-Fas-L Ab or normal IgG was added to the killing test. Interestingly, the Ab slightly, but not significantly, enhanced T cell apoptosis instead of inhibition (Fig. 4E). With a similar killing assay, addition of anti-Gzm C Ab led to a significant reduction in T cell death from 81% to 29% (Fig. 3G). In both cases, IgG controls did not affect the killing. Thus, NK granular cytolytic pathway, but not Fas-L, was the major player in mediating apoptosis in T cells.

Elevated expression of non-classic MHC I RT1CE16 on activated autoreactive T cells coincides with their higher susceptibility to CD8αα$^+$RT1B$^+$Ly49s6$^+$ cell-mediated apoptosis

Since degranulation is triggered by killing stimulatory receptors, we asked if killing stimulatory Ly49s6 on the CD8αα$^+$RT1B$^+$Ly49s6$^+$ cells initiated the killing. It is known that the ligands for Ly49 are non-classic MHC I molecules including RT1CE on the target cells (20, 23). CD8αα homodimer preferentially binds to non-classic MHC I molecules and may serve as a co-receptor (24). Expression of non-classic MHC I gene cluster (25) on glomeruli-infiltrating pan T cells and PBL pan T cells was compared (Fig. 5A). Glomeruli-infiltrating pan T cells were largely CD4$^+$ effector autoreactive T cells. On the other hand, PBL pan T cells were a mixture with a majority being non-activated T cells (Fig. 5B). Both T cell populations expressed the majority of 26 non-classic MHC class I RT1C/E, M/N and S/T genes with RT1CE16 the highest (Fig. 5A). However, glomeruli-infiltrating pan T cells showed a significantly higher level of RT1CE16 than PBMC pan T cells. Elevated level of expression of RT1CE16 in glomeruli-infiltrating T cells was further confirmed by both RT-PCR and qPCR (Fig. 5C, D). We asked if activation led to up-regulation of RT1CE16 in T cells, which made them more susceptible to CD8αα$^+$RT1B$^+$Ly49s6$^+$ cell-induced apoptosis. Resting or activated T cells from three pCol(28–41)-specific autoreactive T cell lines were used for the determination of their RT1CE16 expression with qPCR. First, activated T cells showed a much higher susceptibility to CD8αα$^+$RT1B$^+$Ly49s6$^+$ cell-mediated apoptosis than resting T cells (Fig. 5E). Interestingly, the activated T cells also showed a much higher expression level of RT1CE16 than the resting T cells (Fig. 5F). Susceptibility to apoptosis was positively correlated to RT1CE16 expression level (Fig. 5F). This correlation suggests that RT1CE triggered Ly49s6-mediated degranulation.

Discussion

The CD8αα$^+$RT1B/D$^+$Ly49s6$^+$cell mediates a unique immune tolerance by killing effector T cells in autoimmune target

We have previously reported the CD8αα$^+$RT1B/D$^+$Ly49s6$^+$ cell as a CD8αα$^+$RT1B/D$^+$ dendritic cell-like cell. This cell actively infiltrates inflamed autoimmune target tissue and further induces apoptosis in effector T cells in a rat model for autoimmune glomerulonephritis (13,14). As a result, an on-going autoimmune inflammation in the target is terminated at an early stage without any significant impact on the host (12). Although Ag presentation is a critical step leading to T cell apoptosis, it was not clear which molecule/pathway in this cell actually induced T cell apoptosis. In this study, we not only re-confirmed presence of Ag processing/presenting pathways, but also revealed complicated cytotoxic mechanisms identical to Ly49s$^+$ subset of NK cells in this cell. This cell especially expressed killing stimulatory receptor Ly49s6 with non-classic MHC I RTCE16 on T cells

as a ligand. Cytotoxicity by this cell was eventually mediated by granular cytolytic protein Gzm C, as Ab to Gzm C significantly inhibited its cytotoxicity on T cells. Our results, together with our previous findings, lead to the following scenario (Fig. 5G): the CD8αα$^+$RT1B/D$^+$Ly49s6$^+$ cells actively infiltrate inflamed target tissue, and as a professional APC, they processes and present local autoantigens to autoreactive effector T cells, leading to the coupling between the two. Ly49s6 and CD8αα on this cell serves as killing stimulatory receptor/co-receptor; their binding to non-classic MHC I RT1CE16 on target T cells following the coupling triggers Gzm C mediated cytotoxicity. To our knowledge, only a few, if any, known immune tolerance mechanisms act on a pre-existing autoimmune inflammation. In summary, the CD8αα$^+$RT1B/D$^+$Ly49s6$^+$ cell recognizes target T cells as an APC, and further kills the target in an identical way to a Ly49s$^+$ NK cell. Thus, this is NK-like cell with Ag-presenting capacity. For more accurate description of its unique dual functions, we temporally renamed it to *CD8αα$^+$ Ag presenting-natural killer-like* cells or simply CD8αα$^+$ AP-NK cell (Fig. 5G).

The CD8αα$^+$ AP-NK cell is a novel immune cell with dual functions of APC and NK cell

Both professional APC function and NK toxicity of the CD8αα$^+$ AP-NK cell were required for the selective elimination of effector autoreactive T cells. Several immune cells with dual functions have been reported. However they are functionally and phenotypically different from the CD8αα$^+$ AP-NK cell. Inhibitory Ly49 receptors have been detected on a cell of the myeloid lineage in mice as a trafficking regulator (26). Since these cells lack any NK cytotoxic machineries, they are not truly dually functional. A CD4$^+$CD8$^+$ macrophage is capable of killing tumor cells with NKG2D-Gzm B–dependent mechanism (27). Except for its phenotypic and functional differences from the CD8αα$^+$ AP-NK cell, it remains unclear if this cell is a professional APC, and if both its APC function and NK-like cytotoxicity are required to kill tumors. A special killer DC in spleen has been identified (28). This cell first displays an NK-like capacity with expression of NKG2D/DAP12, and subsequently differentiates into a DC with a loss of NKG2D/DAP12 and diminished killing capacity (28). Thus, its NK and APC function are sequential but not simultaneous as seen in CD8αα$^+$ AP-NK cells. Exact function of this killer DC remains unclear but may provide a link between innate and adaptive immunity. A splenic CD8$^+$ DC has been reported to induce T cell apoptosis with Fas-L (29). Although it seems that APC function is required for recognition of T cells, the killing mechanism is not through NK killing receptor. Thus, the CD8αα$^+$ AP-NK cells are a new type of immune cells with dual functions of professional APC and NK cytotoxicity.

What is the lineage of the CD8αα$^+$ AP-NK cells?

Dual functions of the CD8αα$^+$ AP-NK cells raise an interesting question regarding their lineage. Our earlier studies showed that the cells were derived from bone marrow, and were most likely a phagocytic lineage as they were adhesive, morphologically resembled DC after culture, and expressed professional APC associated genes such as MHC II and invariant chain (14,15). However, our observations in this study suggested otherwise, as the cell possesses a set of NK's cytotoxicity-related molecules, from NK killing receptors, DAP12, Gzms/perforin to Fas-L. However, majority of these molecules are not NK-specific, and may also be expressed by other immune cells (26–29). It is known that dendritic cells can express

some granzymes. In mice, myeloid cells express certain Ly49 isoforms. Myeloid cells in mice and humans express DAP12. Thus, it is not sufficient to conclude their NK-lineage merely based on the expression of these molecules. On the other hand, many recent studies explored whether NK cells express MHC II as an APC in various species. However, it still remains inconclusive. So far as we know, expression of MHC II by rat NK cells has not been reported. A recent study has reported that decidua basalis NK cells can resemble morphology of DC after differentiation into an isoform due to splice variants of killing receptors (30). The killer DC as described above turns out to be a type of an activated NK cell (31). Thus, it cannot be ruled out if the CD8αα$^+$ AP-NK cell is of the NK lineage with gaining of Ag processing/presenting apparatus. More studies are needed.

Unique cytotoxic machinery in the CD8αα$^+$ AP-NK cell

Although the CD8αα$^+$ AP-NK cell possesses similar cytotoxic machinery to Ly49s$^+$ NK cells, there are some differences. *First*, granule cytolytic proteins in NK and CD8$^+$ T cells are mainly Gzm A and B. On the other hand, they were predominantly Gzm C in the CD8αα$^+$ AP-NK cells. Gzm C is much less known. In fact, it remains controversial if natural Gzm C is a monomer or homodimer, or if it has any function beyond allogenic rejection (32–34). An X-ray crystallography on native Gzm C revealed it to be a homodimer (21). Because homodimeric configuration seals its catalytic site, Gzm C needs to be converted to be active (21). Our result supported homodimer configuration. This self-locking mechanism may be necessary to minimize “collateral damage” during killing of effector autoreactive T cells. *Second*, Ly49 is among many NK receptors with MHC class I as ligands. These NK receptors are largely killing inhibitory as a safeguard for self-cells. In contrast, killing stimulatory receptors such as NKG2D bind to other ligands to initiate killing (35). Thus, it seems a paradox why some MHC class I-binding receptors, e.g. stimulatory Ly49s, activate killing. Recent studies have revealed unique functions of these killing stimulatory receptors in allogeneic rejection and certain infections (23, 36). Our discovery adds one more function of these MHC I-binding killing stimulatory receptors in self-immune tolerance: killing “bad” effector autoreactive T cells. Recognition of autoreactive T cells through Ag presentation of the CD8αα$^+$ AP-NK cell, therefore, is necessary to avoid killing other innocent T cells.

Potential significances of the CD8αα$^+$ AP-NK cell

Many tolerance mechanisms *prevent* autoimmunity/inflammation *de novo*. It is less known about the tolerance mechanisms following the occurrence of autoimmune inflammation; these mechanisms must be able to *contain* pre-existing inflammation. The CD8αα$^+$ AP-NK cell-mediated mechanism is one of them. In fact, LEW rats, which are “resistant” to autoimmune glomerulonephritis, do develop disease identical to disease-prone WKY rats (12, 14). However, disease in LEW rats is *contained* at early stages by the CD8αα$^+$ AP-NK cell, rather than *prevented* (12, 13). Due to a full recovery, the hosts do not experience a significant impact of autoimmune inflammation on their health status. Mechanisms for *containing* autoimmune inflammation are as equally critical as those for preventing. Activation of autoreactive T cells during an infection is well known (37, 38). Co-presentation of leaked autoantigens with pathogens during an infection by APC activates autoreactive T cells, which in turn cause autoimmune inflammation at infection site (39).

Yet, infection rarely causes autoimmunity. Beyond many others, one reason may be that micro-scale autoimmunity during an infection is *contained* locally by infiltrating CD8αα$^+$ AP-NK cells. These cells may preferentially kill autoreactive T cells but spare pathogen-specific T cells, because they present much more leaked autoantigens at the infection site. Thus, micro-scale autoimmunity is subsequently terminated without significant impact on the host. *Second*, as the CD8αα$^+$ AP-NK cells are able to actively infiltrate inflamed tissue and further terminate a pre-existing autoimmune inflammation, we are asking if this unique tolerance mechanism may be used for development of immunotherapies for treating pre-existing autoimmune diseases, especially of inflammatory nature.

Acknowledgments

Grant Support: This study was supported by NIH R01-DK60029 and R01-DK077857 (to Y. H. Lou), and an NIH supplemental grant (A. Ross).

Global gene expression detection using DNA microarray was performed at Quantitative Genomics & Microarray Service Center, University of Texas, HSC at Houston. We thank Drs. Tuan Tran for technical help.

Abbreviations used in this paper

Gzm	granzyme
PBMC	peripheral blood mononuclear cells
RT1B/D	rat MHC class II B and D loci
RT1CE	rat non-classic MHC I C/E loci

References

1. Davidson A, Diamond B. Autoimmune Diseases. N Engl J Med. 2001; 345:340–350. [PubMed: 11484692]
2. Condemi JJ. The autoimmune diseases. JAMA. 1992; 268:2882–2892. [PubMed: 1433704]
3. Ohashi PS. T-cell signalling and autoimmunity: molecular mechanisms of disease. Nat Rev Immunol. 2002; 2:427–438. [PubMed: 12093009]
4. Maddur MS, Miossec P, Kaveri SV, Bayry J. Th17 cells: biology, pathogenesis of autoimmune and inflammatory diseases, and therapeutic strategies. Am J Pathol. 2012; 181:8–18. [PubMed: 22640807]
5. Feldmann M, Steinman L. Design of effective immunotherapy for human autoimmunity. Nature. 2005; 435:612–619. [PubMed: 15931214]
6. Sakaguchi S, Sakaguchi N, Shimizu J, Yamazaki S, Sakihama T, Itoh M, Kuniyasu Y, Nomura T, Toda M, Takahashi T. Immunologic tolerance maintained by CD25$^+$CD4$^+$ regulatory T cells: their common role in controlling autoimmunity, tumor immunity, and transplantation tolerance. Immunol Rev. 2001; 182:18–32. [PubMed: 11722621]
7. Morel PA, Feili-Hariri M, Coates PT, Thomson AW. Dendritic cells, T cell tolerance and therapy of adverse immune reactions. Clin Exp Immunol. 2003; 133:1–10. [PubMed: 12823271]
8. Rutella S, Danese S, Leone G. Tolerogenic dendritic cells: cytokine modulation comes of age. Blood. 2006; 108:1435–1440. [PubMed: 16684955]
9. Setiady YY, Pramoonjago P, Tung KS. Requirements of NK cells and proinflammatory cytokines in T cell-dependent neonatal autoimmune ovarian disease triggered by immune complex. J Immunol. 2004; 173:1051–1058. [PubMed: 15240693]
10. Albert LJ, Inman RD. Molecular Mimicry and autoimmunity. N Engl J Med. 1999; 341:2068–2074. [PubMed: 10615080]

11. Horwitz MS, Bradley LM, Harbertson J, Krahl T, Lee J, Sarvennick N. Diabetes induced by Coxsackie virus: Initiation by bystander damage and not molecular mimicry. Nat Med. 1998; 4:781–785. [PubMed: 9662368]
12. Robertson J, Wu J, Arends J, Zhou C, Adrogue HE, Chan JT, Lou YH. Spontaneous recovery from early glomerular inflammation is associated with resistance to anti-GBM glomerulonephritis: tolerance and autoimmune tissue injury. J Autoimmunity. 2008; 30:246–256. [PubMed: 18054199]
13. Zhou C, Robertson J, Wu J, Bartkowiak T, Parker K, McMahon J, Lou YH. Natural recovery from anti-GBM glomerulonephritis is associated with glomeruli-infiltrating $CD8\alpha^{+}CD11c^{+}$MHC class-II^{+} cells. Am J Nephrol. 2011; 34:519–528. [PubMed: 22068125]
14. Wu J, Zhou C, Robertson J, Weng CCY, Meistrich ML, Tailor RC, Lou YH. Identification of a bone marrow derived $CD8\alpha\alpha^{+}$ dendritic cell like population in inflamed autoimmune target tissue with capability of inducing T cell apoptosis. J Leukoc Biol. 2010; 88:849–861. [PubMed: 20628068]
15. Wu J, Zhou C, Robertson J, Carlock C, Lou YH. A peripheral blood $CD8\alpha\alpha^{+}CD11c^{+}$MHC-$II^{+}$ cell attenuates autoimmune glomerulonephritis in rats. Kidney Intl. 2014; 85:1078–1090.
16. Wu J, Cherwinski H, Spies T, Phillips JH, Lanier LL. DAP10 and DAP12 form distinct, but functionally cooperative, receptor complexes in natural killer cells. J Exp Med. 2000; 192:1059–1068. [PubMed: 11015446]
17. Warren HS, Smyth MJ. NK cells and apoptosis. Immunol Cell Biol. 1999; 77:64–75. [PubMed: 10101688]
18. Kveberg L, Jiménez-Royo P, Naper C, Rolstad B, Butcher GW, Vaage JT, Inngjerdingen M. Two complementary rat NK cell subsets, $Ly49s3^{+}$ and NKR-$P1B^{+}$, differ in phenotypic characteristics and responsiveness to cytokines. J Leukoc Biol. 2010; 88:87–93. [PubMed: 20395458]
19. Nylenna O, Naper C, Vaage JT, Woon PY, Gauguier D, Dissen E, Ryan JC, Fossum S. The genes and gene organization of the Ly49 region of the rat natural killer cell gene complex. Eur J Immunol. 2005; 35:261–272. [PubMed: 15593300]
20. Naper C, Dai KZ, Kveberg L, Rolstad B, Niemi EC, Vaage JT, Ryan JC. Two structurally related rat Ly49 receptors with opposing functions (Ly49 stimulatory receptor 5 and Ly49 inhibitory receptor 5) recognize nonclassical MHC class Ib-encoded target ligands. J Immunol. 2005; 174:2702–2711. [PubMed: 15728478]
21. Kaiserman D, Buckle AM, Van Damme P, Irving JA, Law RH, Matthews AY, Bashtannyk-Puhalovich T, Langendorf C, Thompson P, Vandekerckhove J, Gevaert K, Whisstock JC, Bird PI. Structure of granzyme C reveals an unusual mechanism of protease autoinhibition. Proc Natl Acad Sci USA. 2009; 106:5587–5592. [PubMed: 19299505]
22. Lettau M, Paulsen M, Kabelitz D, Janssem O. Storage, expression and function of Fas ligand, the key death factor of immune cells. Curr Med Chem. 2008; 15:1684–1696. [PubMed: 18673218]
23. Shegarfi H, Dai KZ, Daws MR, Ryan JC, Vaage JT, Rolstad B, Naper C. The rat NK cell receptors Ly49s4 and Ly49i4 recognize nonclassical MHC-I molecules on Listeria monocytogenes-infected macrophages. J Leukoc Biol. 2011; 89:617–623. [PubMed: 21248147]
24. Gao GF, Willcox BE, Wyer JR, Boulter JM, O'Callaghan CA, Maenaka K, Stuart DI, Jones EY, Van Der Merwe PA, Bell JI, Jakobsen BK. Classical and nonclassical class I major histocompatibility complex molecules exhibit subtle conformational differences that affect binding to $CD8\alpha\alpha$. J Biol Chem. 2000; 275:15232–15238. [PubMed: 10809759]
25. Roos C, Walter L. Considerable haplotypic diversity in the RT1-CE class I gene region of the rat major histocompatibility complex. Immunogenetics. 2004; 56:773–777. [PubMed: 15578174]
26. Sasawatari S, Yoshizaki M, Taya C, Tazawa A, Furuyama-Tanaka K, Yonekawa H, Dohi T, Makrigiannis AP, Sasazuki T, Inaba K, Toyama-Sorimachi N. The Ly49Q receptor plays a crucial role in neutrophil polarization and migration by regulating raft trafficking. Immunity. 2010; 32:200–213. [PubMed: 20153219]
27. Baba T, Iwasaki S, Maruoka T, Suzuki A, Tomaru U, Ikeda H, Yoshiki T, Kasahara M, Ishizu A. Rat $CD4^{+}CD8^{+}$ macrophages kill tumor cells through an NKG2D- and granzyme/perforin-dependent mechanism. J Immunol. 2008; 180:2999–3006. [PubMed: 18292522]

28. Chan CW, Crafton E, Fan HN, Flook J, Yoshimura K, Skarica M, Brockstedt D, Dubensky TW, Stins MF, Lanier LL, Pardoll DM, Housseau F. Interferon-producing killer dendritic cells provide a link between innate and adaptive immunity. Nat Med. 2006; 12:207–213. [PubMed: 16444266]
29. Suss G, Shortman K. A subclass of dendritic cells kills CD4 T cells via Fas/Fas-ligand-induced apoptosis. J Exp Med. 1996; 183:1789–1796. [PubMed: 8666935]
30. Siewiera J, Gouilly J, Hocine HR, Cartron G, Levy C, Al-Daccak R, Jabrane-Ferrat N. Natural cytotoxicity receptor splice variants orchestrate the distinct functions of human natural killer cell subtypes. Nat Commun. 2015; :6.doi: 10.1038/ncomms10183
31. Vosshenrich C, Lesjean-Pottier S, Hasan M, Richard-Le Goff O, Corcuff E, Mandelboim O, Di Santo JP. CD11cloB220^{+} interferon-producing killer dendritic cells are activated natural killer cells. J Exp Med. 2007; 204:2569–2578. [PubMed: 17923507]
32. Getachew Y, Stout-Delgado H, Miller BC, Thiele D. Granzyme C supports efficient CTL-mediated killing late in primary alloimmune response. J Immunol. 2008; 181:7810–7817. [PubMed: 19017970]
33. Cai SF, Fehniger TA, Cao X, Mayer JC, Brune JD, French AR, Ley TJ. Differential expression of granzyme B and C in murine cytotoxic lymphocytes. J Immunol. 2009; 182:6287–6297. [PubMed: 19414782]
34. Bailey NC, Kelly CJ. Nephritogenic T cells use granzyme C as a cytotoxic mediator. Eur J Immunol. 1997; 27:2302–2309. [PubMed: 9341773]
35. Eric OL, Kim H, Liu D, Peterson ME, Rajagopalan S. Controlling natural killer cell responses: integration of signals for activation and inhibition. Ann Rev Immunol. 2013; 31:227–258. [PubMed: 23516982]
36. Sivori S, Carlomagno S, Falco M, Romeo E, Moretta L, Moretta A. Natural killer cells expressing the KIR2DS1-activating receptor efficiently kill T-cell blasts and dendritic cells: implications in haploidentical HSCT. Blood. 2011; 117:4284–4292. [PubMed: 21355085]
37. Wucherpfennig KW. Mechanisms for the induction of autoimmunity by infectious agents. J Clin Invest. 2001; 108:1097–1104. [PubMed: 11602615]
38. Fujinami RS, von Herrath MG, Christen U, Whitton JL. Molecular mimicry, bystander activation, or viral persistence: infections and autoimmune disease. Clin Microbiol Rev. 2006; 19:80–94. [PubMed: 16418524]
39. Horwitz MS, Ilic A, Fine C, Rodriguez E, Sarvetnick N. Presented antigen from damaged pancreatic β cells activates autoreactive T cells in virus-mediated autoimmune diabetes. J Clin Invest. 2002; 109:79–87. [PubMed: 11781353]

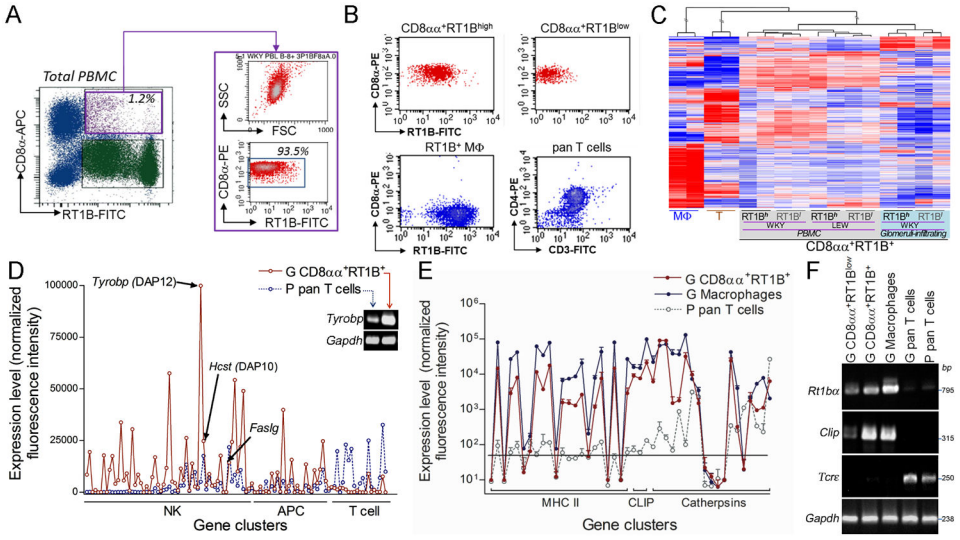

FIGURE 1.

CD8αα$^+$RT1B/D$^+$ cells express both genes associated with professional antigen processing/presenting and NK cytotoxicity. (**A**) Multi-color flow cytometry analyses show a CD8αα$^+$RT1B/D$^+$ population (purple gate on RT1B-FITC vs CD8α-APC plot, left panel) in rat peripheral blood mononuclear cells (PBMC); right panel shows purified CD8αα$^+$RT1B/D$^+$ population as shown by both SSC vs FSC and CD8α vs RT1B/D plot. (**B**) Representative flow cytometric plots show each isolated population from glomeruli infiltrating leukocytes as indicated on the top of each plot. MΦ, macrophages. (**C**) A representative clustering analysis based on DNA microarray shows similar global gene expression patterns among all CD8αα$^+$RT1B/D$^+$ subpopulations from different sources in both LEW and WKY rats; glomeruli-infiltrating macrophages (MΦ) and pan T cells are shown as controls. (**D**) Summary of expressions of gene clusters associated with NK cells, APCs and T cells. n=4. *Inset*, RT-PCR detection of *Tyrobp* and control house keeper gene *Gapdh.* (**E**) Summary of expressions of genes associated with Ag processing/presentation for professional APCs; expression levels in (**D**) and (**E**) are mean normalized intensities for each gene in DNA microarray. n=4. (**F**) A representative RT-PCR shows expression of Ag presenting related α chain of rat MHC class II RT1B (*Rt1bα*) and invariant chain (*Clip*) in various cell populations as indicated; TcR ε chain (*Tcrε*) and *Gapdh* were used as controls.

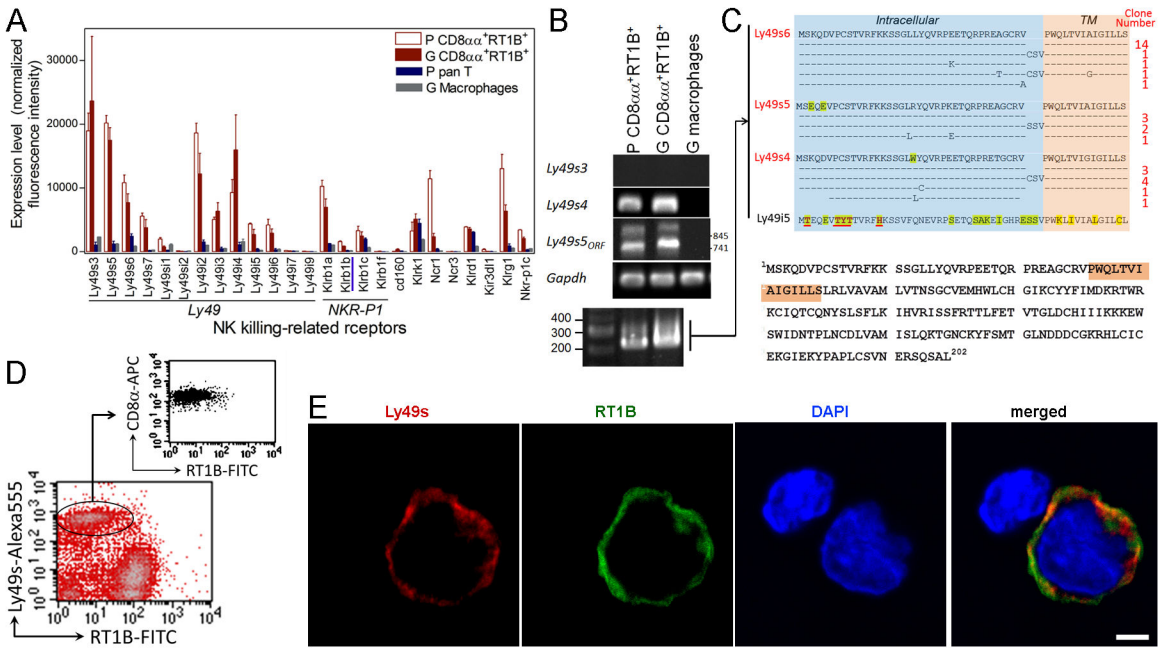

FIGURE 2.

CD8αα$^+$RT1B/D$^+$ cells express NK killing stimulatory receptors Ly49s6. (**A**) DNA microarray shows expression of various NK receptors in PBMC (P) and glomeruli-infiltrating (G) CD8αα$^+$RT1B/D$^+$ cells, but not in control PBMC T cells and glomeruli-infiltrating macrophages; NK receptor genes are grouped; gene *Klrb1a* which encodes hallmark of an NK subset NKR-P1B is underlined; note that many Ly49 members were not covered by DNA microarray. (**B**) RT-PCR detection of mRNAs for representative Ly49 receptors in the indicated cell populations; lower panel shows degenerative PCR products for transmembrane (TM) and intracellular fragment of Ly49 in glomeruli-infiltrating CD8αα$^+$RT1B/D$^+$ cells. (**C**) Alignment of a.a. sequences of cloned cDNA from degenerative PCR (see lower panel in (**B**) as connected by lines) demonstrates expression of mainly killing stimulatory receptors in CD8αα$^+$RT1B/D$^+$ cells; numbers of clones for each sequence are indicated at the right with majority of them being Ly49s6; inhibitory motif in intracellular fragment of Ly49 is underlined in red at the bottom; *TM*, transmembrane. Lower panel shows a.a. sequence of cloned Ly49s6 with transmembrane domain shadowed. (**D**) Three-color flow cytometry on glomeruli-infiltrating leukocytes after removal of pan T cells shows a RT1B/D$^+$Ly49s6$^+$ population (lower panel) which is also CD8α$^+$ (upper panel for the gated population in lower panel). (**E**) Immunofluorescence shows expression of both Ly49s6 (red) and RT1B (green) on a CD8αα$^+$RT1B/D$^+$ cell; a nearby T cell is shown as an internal control for staining. bar= 3μm

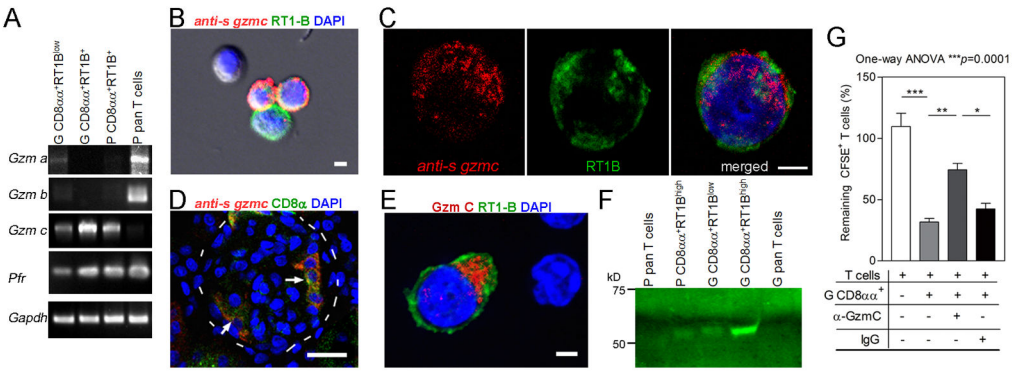

FIGURE 3.

Granule cytolytic granzyme C (Gzm C) in CD8αα$^+$RT1B/D$^+$Ly49s$^+$ cells mediates killing of autoreactive effector T cells. (**A**) RT-PCR detection of granule cytolytic proteins in various cell populations. G, glomeruli-infiltrating; P, PBMC; *Gzm*, granzyme; *Pfr*, perforin. (**B** and **C**) Combination of immunofluorescence on RT1B (green) and ISH with full length *gzmc* antisense RNA (anti-s) as a probe (red) demonstrate *gzmc* mRNA in PBMC CD8αα$^+$RT1B/D$^+$Ly49s6$^+$ cells; cells probed with sense RNA were negative. In (**B**), one double negative and one single RT1B/D$^+$ cell (green) are shown as internal controls. Bars=3 μm. (**D**) Immunofluorescence/ISH shows *gzmc* mRNA in CD8αα$^+$RT1B/D$^+$Ly49$^+$ cells (arrows) in glomeruli (outlined by dash line) of an immunized rat. Bar=30μm. (**E**) Immunofluorescence shows cytoplasmic Gzm C (red) in a glomeruli-infiltrating CD8αα$^+$RT1B/D$^+$Ly49s$^+$ cell (green); two nearby double negative T cells are shown as internal controls. Bar = 3 μm. (**F**) Western Blot on the proteins from various cells shows Gzm C of 56kD in CD8αα$^+$RT1B/D$^+$Ly49s$^+$ cells but not in T cells. (**G**) Killing assay under various conditions as indicated shows reduced killing efficacy of target T cells in the presence of anti-Gzm C Ab (α-Gzm C). Glomeruli-infiltrating CD8αα$^+$RT1B/D$^+$Ly49s$^+$ cells (G CD8αα$^+$) were used as killing effectors and pCol(28–41)-specific T cells as targets. Killing was expressed as % of CFSE-labeled target T cells in control wells without killing effectors. Three independent experiments were conducted with similar results. One-way ANOVA with Tukey post test was performed. *, $p<0.05$, **, $p<0.01$, ***, $p<0.001$.

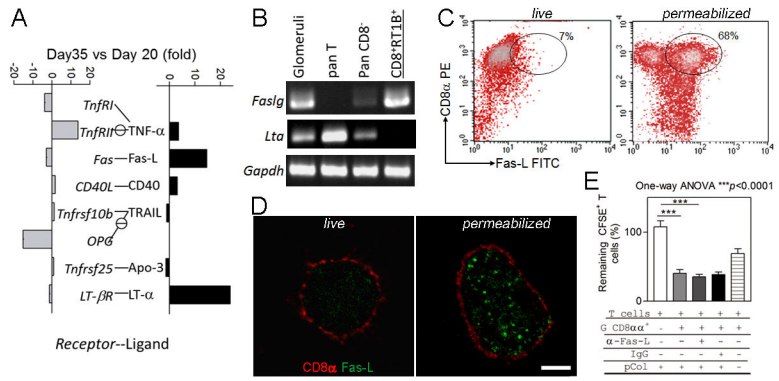

FIGURE 4.

CD8αα$^+$RT1B/D$^+$Ly49s6$^+$ cells express intracellular Fas-L. (**A**) qPCR array for apoptosis pathway on glomerular mRNAs at early inflammation (day 20 post immunization) and T cell apoptosis peak (day 35) of immunized WKY rats; apoptosis-inducing receptors and ligands are shown separately and paired; expression of each gene is expressed as fold changes between day 20 and day 35; note that significant increases are seen in both *Faslg* and *Lta*. (**B**) RT-PCR shows the detection of a high level of *Faslg* mRNA in the isolated glomeruli-infiltrating CD8αα$^+$RT1B/D$^+$Ly49s$^+$ cells (CD8$^+$RT1B$^+$), but no *Lta* expression was detected. (**C**) Two color flow cytometry on isolated glomeruli-infiltrating CD8αα$^+$RT1B/D$^+$Ly49s6$^+$ cells for the detection of Fas-L; permeabilized cells showed a Fas-L$^+$CD8α$^+$ population (gated). (**D**) Immunofluorescence shows intracellular Fas-L (green) in a permeabilized CD8αα$^+$RT1B/D$^+$ cell (red) (right panel), but not in a live one (left panel). Bar =3 μm. (**E**) Killing assay shows that addition of Fas-L Ab (α-Fas-L) did not inhibit CD8αα$^+$RT1B/D$^+$Ly49s6$^+$ cell-mediated killing of pCol(28–40) specific T cells. Three independent experiments were conducted with similar results. One-way ANOVA with Tukey post test was conducted. ***, p<0.001.

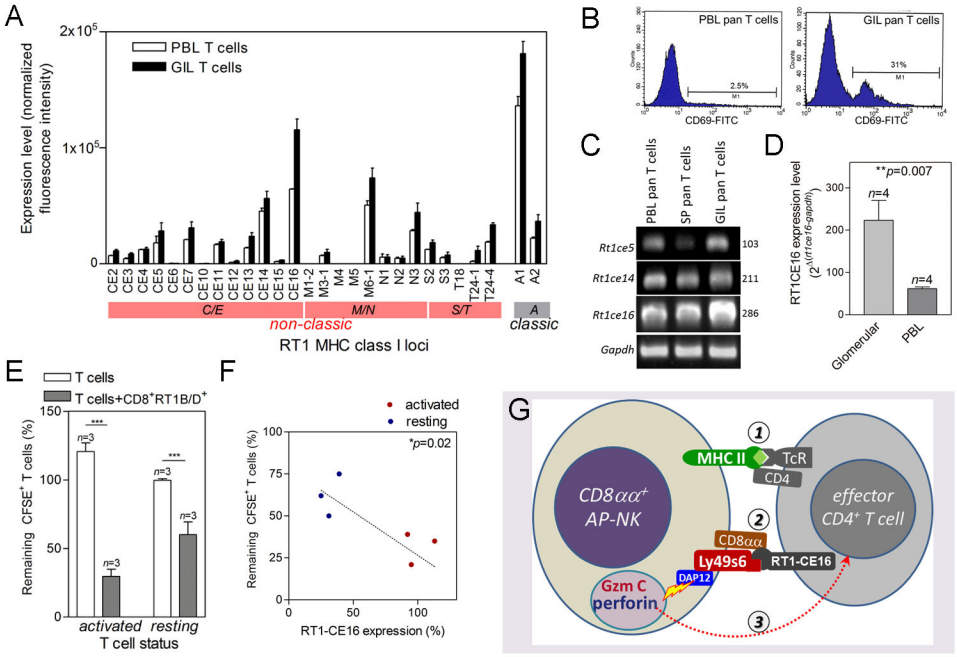

FIGURE 5.

Activated autoreactive T cells with elevated level of RT1CE16 are more susceptible to the killing by CD8αα$^+$RT1B/D$^+$Ly49s6$^+$ cells. (**A**) Summary of classic (RT1A) and non-classic (RT1C/E, M/N and S/T) MHC class I gene cluster expression pattern in PBMC (P) and glomeruli-infiltrating (GIL) T cells; expression level is normalized intensities in DNA microarray. *n*=4. (**B**) Flow cytometry shows detection of T cell activation marker CD69 in PBL pan T cells or glomeruli-infiltrating T cells as indicated. (**C**) Conventional RT-PCR detection of representative non-classic MHC I genes in PBL, splenic (SP), and glomeruli-infiltrating T cells. (**D**) Quantitative PCR detection of *Rt1ce16* expression in glomeruli-infiltrating or PBL T cells. Relative expression levels to house-keeping gene *Gapdh* are shown. (**E**) Summary of susceptibility of T cells to CD8αα$^+$RT1B/D$^+$Ly49s6$^+$ cell-mediated killing. Killing efficacy is expressed as % of remaining CFSE-labeled target T cells. T cells alone were used as control. (**F**) Correlation between RT1CE16 expression level in resting and activated pCol(28–40)-specific T cell lines and their susceptibilities to CD8αα$^+$RT1B/D$^+$Ly49s6$^+$ cell-mediated killing; RT1CE16 expression levels were measured by qPCR and expressed as % of average for activated T cells; linear progression was calculated; each sample was duplicated. (**G**) Schematic diagram depicts three-step killing of autoreactive T cells by CD8αα$^+$RT1B/D$^+$Ly49s6$^+$ cells (renamed to CD8αα$^+$ AP-NK cell): *Step 1*, Coupling of CD8αα$^+$ AP-NK cell with effector autoreactive T cell through its Ag presentation. *Step 2*, Binding of Ly49s/CD8αα on CD8αα$^+$ AP-NK cell to RT1CE16 on the T cell. *Step 3*, DAP12 mediated release of granule cytotoxic proteins Gzm C and perforin from CD8αα$^+$ AP-NK cell, which induce apoptosis in the target T cell.

Table 1

List of PCR primers for detection various gene expression or cloning of cDNAs.

Rat gene	Primers	Product size (*bp*)
Rt1ba	F, 5′-AGAACAGAGATGCCGCTCAGCAGAGC-3′ R, 5′-TTCCCAGGATGGTACTCAAAGGGGCC-3′	795
Clip (Il)	F, 5′-TGTTCTTGTGAAGACAGAAGCCAGC-3′ >R, 5′-GTATCCAGCCTAGATTAAGGGTAGG-3′	315
Tcrɛ	F, 5′-GGTACTGGTGGCAGGCCCAGAGG-3′ R, 5′-GTTCTAGGATGCGTGTTCACCAGG-3′	250
Gapdh	F, 5′-CTTCACCACCATGGAGAAGGC-3′ R, 5′-GGCATGGACTGTGGTCATGAG-3′	238
Tyrobp	F, 5′-GCTTCAGGGTCAGAGGCCAGAA-3′ R, 5′-TGGGGACAGAAACGGTACAAGG-3′	218
Ly49s3	F, 5′-GTCTGTATTTCAGTATGTCAGG-3′ R, 5′-ATTCTCCACATGCAAGCTCCTC-3′	236
Ly49s4	F, 5′-GTATGTATTTCAGTATGTCAGG-3′ R, 5′-TCACACAGCAGAATGTGACC-3′	135
$Ly49s5_{ORF}$	F, 5′-TCCCAAAATGAGTAAGCAGGATG-3′ R, 5′-ATCATCTCTCTATTCACACAGCAG-3′	854/741
Ly49s6	F, 5′-CTCCCAAAATGAGTAAGCAGG-3′ R, 5′-CATCTCTTTATTCACAGAGCAG-3′	614
$Ly49_{TM/IC}$	F, 5′-ACAGACTTCATACATCATTCCC-3′ R, 5′-AACAGCAACCAGCCGAAG-3′	199/208
Gzma	F, 5′-CTGGGTGTCCTCTCTTACTACTGTC-3′ R, 5′-TTAAACAGCGCCCTTCGCAGTCTTC-3′	766
Gzmb	F, 5′-TTTCCTAGAGGTGAAGAGAGCAAGG-3′ R, 5′-AGGGCAGATGGTTAGTCAGGAAATG-3′	860
$Gzmc_{ORF}$	F, 5′-GAGGATGCCACCAGTCCTGATACTC-3′ R, 5′-GCTATAGGGAAGATGGTTAGTCAGG-3′	800
Pfr	F, 5′-CTCAAGCGAATACAAAGCTTGCGAGG-3′ R, 5′-TTGTTTTTACCACACAGCCCCACTGC-3′	859
Rt1ce5	F, 5′-CCTTCCACATTCAACCTTGCTG-3′ R, 5′-TGTAGAAGTGAGGAGTTGCAG-3′	103
Rt1ce14	F, 5′-CCTTCCAGAAGTGGGCATCTGT-3′ R, 5′-ATGGCCACAGCTCCAATGATGG-3′	211
Rt1ce16	F, 5′-GCAGTTGAATGGGGAGGACC-3′ R, 5′-ATCACAACAGCCACCACAGC-3′	286
Faslg	F, 5′-AAAGACCACAAGGTCCAACA-3′ R, 5′-AGTCTCTAGCTTATCCCATGA-3′	341
Lat	F, 5′-CCCACACAGAC GGCATCTCC-3′ R, 5′-CTGAGCATCTGGAGTGGCCC-3′	210

F, forward; **R**, reversed